Target Tracking via Recursive Bayesian State Estimation in Radar Networks

Yijian Xiang*, Murat Akcakaya†, Satyabrata Sen‡, Deniz Erdogmus§, and Arye Nehorai*

*Department of Electrical and Systems Engineering, Washington University in St. Louis, St. Louis, MO 63130 USA
Email: yijian.xiang@wustl.edu, nehorai@ese.wustl.edu

†Department of Electrical and Computer Engineering, University of Pittsburgh, Pittsburgh, PA 15213 USA
Email: akcakaya@pitt.edu

‡Computational Sciences and Engineering Division, Oak Ridge National Laboratory, Oak Ridge, TN 37831 USA
Email: sens@ornl.gov

§Department of Electrical and Computer Engineering, Northeastern University, Boston, MA 02115 USA
Email: erdogmus@ece.neu.edu

***Abstract*—Modern cognitive radar networks incorporating intelligent and cognitive support-modules can actively adjust the radar-target geometry and optimally select a subset of radars to track the target of interest. Based on the theories of dynamic graphical model (DGM) and recursive Bayesian state estimation (RBSE), we propose a framework for single target tracking in mobile and cooperative radar networks, jointly considering path planning and radar selection. We formulate the tracking procedure as two iterative steps: (i) solving a combinatorial problem based on the expected cross-entropy measure to select the optimal subset of radars and their locations, and (ii) tracking the target using RBSE technique. We simulate the proposed framework using an illustrative example in 2-D space and demonstrate the tracking performance.**

I. Introduction

Target tracking in complicated environments and in the presence of stealthy targets is becoming one of the most challenging problems in radar systems. The goal of target tracking is to extract the target state information (e.g., position and velocity) from received measurements, which are often corrupted by unwanted clutter and noise, and assumed target kinematic models. With remarkable advances in sensor techniques [1], it is much more prevalent nowadays to deploy radars on mobile platforms, such as self-controlled and self-tasked unmanned aerial vehicles (UAVs), to form a mobile radar network and cooperatively track the target. This type of radar networks provide additional degrees of freedom for the radars to interrogate the target from different perspectives.

To achieve great tracking accuracy, it is imperative for radar networks to incorporate intelligent and cognition cycles to fully extract and exploit the environmental information, and optimally manage the available resources [2], [3]. Therefore, a cognitive radar network should be extended to incorporate two key components: (i) *radar selection*, and (ii) *path planning*. In other words, the network can actively select a subset of radars according to certain resource constraints, and plan their trajectories to receive the most informative measurements, which are then used to update the target state with high accuracy.

In existing literature, several radar (sensor) selection methods are proposed to assign radars to operate in a geometry-fixed network [4]–[10]. As radar selection is a combinatorial optimization problem, which is NP-hard in the most scenarios, relaxations are usually applied to obtain a sub-optimal solution. For example, the work in [4] relaxes the problem to a convex optimization problem and uses a heuristic searching method to achieve a feasible solution. The radar selection problem is also cast as a submodular set optimization problem [5], which can be solved by a greedy method with a guaranteed performance. Further, linear programming and semi-definite programming (SDP) approximations are proposed in [8] to reformulate the problems with generalized information measure.

Path planning is a fundamental and relevant topic in automatic control and robotics [11]. For radars (sensors) installed on mobile platforms, it is of great interest to steer the radars to the optimal locations to collect the most informative measurements and gain accurate localization and tracking performance [12]–[19]. To design non-myopic path planning algorithms, several work investigate the policies based on maximizing the determinant of the Fisher information matrix [12], [14], [18], while the work in [16] and [11] adopt information-theoretic objective functions. A partially observable Markov decision process (POMDP) framework is developed in [17] to take into account the expected cumulative cost from the future. However, it remains a challenging issue to find an optimal and efficient policy that can fully explore and exploit the environmental information.

Thus, radar selection and path planning are separately addressed in the existing work, as mentioned above. However, in cognitive radar network, we are motivated to *jointly* consider

The work was supported by AFOSR under Grant No. FA9550-16-1-0386. The work of Sen was performed at the Oak Ridge National Laboratory, managed by UT-Battelle, LLC, for the U.S. Department of Energy, under Contract DE-AC05-00OR22725.

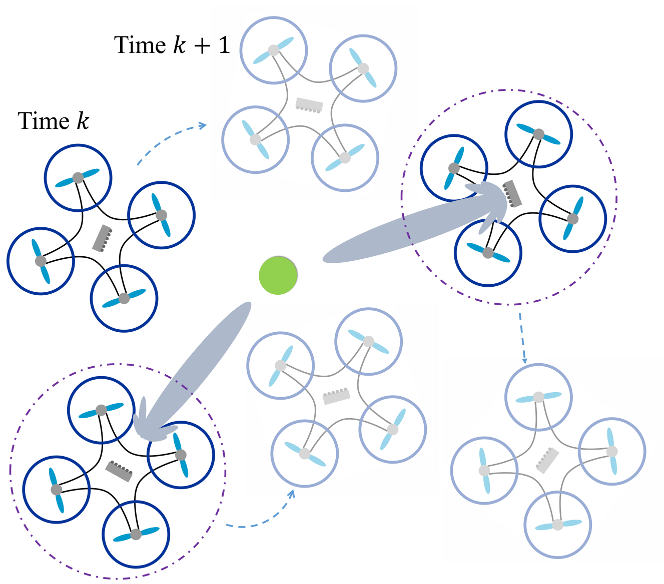

Fig. 1. A cognitive radar network formed by three UAVs with radar selection and path planning strategies. Two circled UAVs are chosen to operate at time k, and the semitransparent UAVs indicate the radar-network geometry structure at time $k+1$.

these two techniques, incorporate them into the cognition cycle, and benefit from this extension. In this paper, we propose a framework for single target tracking based on the theories of dynamic graphical model (DGM) and recursive Bayesian state estimation (RBSE), while jointly considering radar selection and path planning. We formulate the tracking procedure as two iterative steps: (i) solving a combinatorial problem based on the expected negative cross-entropy measure to select the optimal subset of radars and their locations, and (ii) tracking the target using RBSE technique. We demonstrate the proposed method via an illustrative example in 2-D space and achieve good tracking performances.

The rest of paper is organized as follows. In Section II, we introduce the proposed framework of single target tracking in cognitive radar networks. The simulation setup of an illustrative example and the tracking results are described in Section III. Finally, in Section IV, our contributions are summarized and the future work is discussed.

II. Target Tracking Framework in Cognitive Radar Networks

The target tracking framework with a radar network consisting of UAVs is illustrated in Fig. 1. The cooperative radar system decides the optimal subset of radars to operate and their locations at every tracking step, according to some predefined resource management constraints and a well-designed objective function.

The evolution of the target state and its dependence on the kinematic model and on the history information is shown in Fig. 2. The notations are defined as follows:

- Target state at time k is denoted by $\boldsymbol{x}_k$ (e.g., target positions and velocities). The state evolves according to a kinematic model, which is modeled as an order-1 Markov process. The estimation of the state $\boldsymbol{x}_k$ is also dependent on the received measurements at time k and those in history.
- Dictionary $\mathcal{D} = \{\mathcal{D}^s, \mathcal{D}^p\}$ contains the all the possible radars in use in the network (i.e., $\mathcal{D}^s$), and all the discretized positions that radars can arrive in the surveillance region (i.e., $\mathcal{D}^p$) for time k.
- Index set $\mathcal{U}_k = \{\mathcal{U}_k^s, \mathcal{U}_k^p\}$ indicates the selected radars and the planned positions for radars in the network.
- Noisy measurements of the hidden state $\boldsymbol{x}_k$ at time k are denoted by $\mathcal{Z}_k$, when $\mathcal{D}(\mathcal{U}_k)$ is applied.

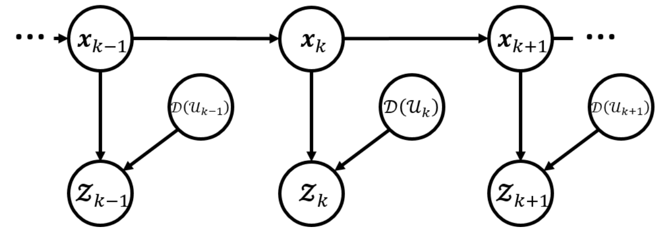

Fig. 2. Graphical model: The evolution of the target state $\boldsymbol{x}_k$ is dependent on the kinematic model mapping from $\boldsymbol{x}_{k-1}$. Here $\mathcal{D}(\mathcal{U}_k)$ indicates the selected radars and their positions; $\mathcal{Z}_k$ denotes noisy measurements of the state $\boldsymbol{x}_k$ if $\mathcal{D}(\mathcal{U}_k)$ is applied.

The graphical model can be expanded to include statistical environmental information, such as a pre-learned geographical model that affects the evolving procedure from $\boldsymbol{x}_{k-1}$ to $\boldsymbol{x}_k$. In this paper, we consider only the effects of the assumed kinematic model.

A. Kinematic Model

In this paper, we consider a 2-D case and use a nearly constant velocity model [20], i.e.,

$$\boldsymbol{x}_{k+1} = \boldsymbol{A}_k \boldsymbol{x}_k + \boldsymbol{v}_k, \tag{1}$$

where the target state is $\boldsymbol{x}_k = [x_k, \dot{x}_k, y_k, \dot{y}_k]^\top$, with x_k and y_k are target positions of x and y directions, respectively, and $\dot{x}_k$ and $\dot{y}_k$ are velocities; and the process noise $\boldsymbol{v}_k$ is modeled as a white Gaussian noise. Further, the transition matrix $\boldsymbol{A}_k$ is given by

$$\boldsymbol{A}_k = \boldsymbol{I}_2 \otimes \bar{\boldsymbol{A}}_k, \tag{2}$$

$$\bar{\boldsymbol{A}}_k = \begin{bmatrix} 1 & T_{\text{in},k} \\ 0 & 1 \end{bmatrix}, \tag{3}$$

where $\boldsymbol{I}_2$ is a 2×2 identity matrix; $\otimes$ is the Kronecker product; and $T_{\text{in},k}$ is the time interval between two consecutive tracking steps. For the process noise, which models the small perturbations on target velocities, we have

$$\mathbb{E}(\boldsymbol{v}_k) = \boldsymbol{0}, \tag{4}$$

$$\mathbb{E}(\boldsymbol{v}_k \boldsymbol{v}_j^\top) = \boldsymbol{V}_k \delta_{kj}, \tag{5}$$

where δ_{kj} is the Kronecker delta function; and the noise covariance matrix is

$$\boldsymbol{V}_k = \text{diag}(q_1, q_2) \otimes \begin{bmatrix} \frac{1}{3}T_{\text{in},k}^4 & \frac{1}{2}T_{\text{in},k}^3 \\ \frac{1}{2}T_{\text{in},k}^3 & T_{\text{in},k}^2 \end{bmatrix}, \tag{6}$$

with q_1 and q_2 denoting the process noise intensities of the x and y directions, respectively.

B. Measurement Model

For simplicity, we consider a linear measurement model. For i_{th} selected radar, we have

$$\boldsymbol{z}_k^{(i)} = \boldsymbol{H}_k^{(i)}(\mathcal{D}(\mathcal{U}_k), \boldsymbol{x}_k)\boldsymbol{x}_k + \boldsymbol{n}_k^{(i)}, \tag{7}$$

where $\boldsymbol{n}_k$ is the zero mean white Gaussian measurement noise; and $\boldsymbol{z}_k$ is the noisy measurement. In addition, the observation matrix is defined as

$$\boldsymbol{H}_k^{(i)}(\mathcal{D}(\mathcal{U}_k), \boldsymbol{x}_k) = \begin{cases} \begin{bmatrix} 1 & 0 & 0 & 0 \\ 0 & 0 & 1 & 0 \end{bmatrix} & \text{if scenario 1} \\ \quad\quad \boldsymbol{0} & \text{if scenario 2} \end{cases}, \tag{8}$$

where scenario 1 indicates that the i_{th} radar can see the target or the beam of the radar cover the target; while scenario 2 indicates that the radar does not receive any echo scattered back from the target. The scenario is determined by the selected radar and its geometry with respect to the target, i.e., $\mathcal{D}(\mathcal{U}_k)$. Further, as can be seen from (8), only positions are measured by radars for scenario 1.

The measurements available for the radar network can be expressed as

$$\begin{aligned} \boldsymbol{z}_k = \text{vec}\mathcal{Z}_k &= \text{vec}\{\boldsymbol{z}_k^{(i)} \mid i \in \mathcal{U}_k^s\} \\ &= \text{vec}\{\boldsymbol{H}_k^{(i)}(\mathcal{D}(\mathcal{U}_k), \boldsymbol{x}_k)\boldsymbol{x}_k + \boldsymbol{n}_k^{(i)} \mid i \in \mathcal{U}_k^s\} \\ &= \boldsymbol{H}_k(\mathcal{D}(\mathcal{U}_k), \boldsymbol{x}_k)\boldsymbol{x}_k + \boldsymbol{n}_k, \end{aligned} \tag{9}$$

where vec operator lumps the elements in a set into a vector; and $\mathcal{U}_k^s$ is the index set that indicates the selected radars. Further, for the measurement noise, we have

$$\mathbb{E}(\boldsymbol{n}_k) = \boldsymbol{0}, \tag{10}$$

$$\mathbb{E}(\boldsymbol{n}_k \boldsymbol{n}_j^\top) = \boldsymbol{R}_k \delta_{kj}. \tag{11}$$

C. Recursive Bayesian Estimation

As the linear models are considered for the kinematic model and the measurement model, we apply Kalman filter to recursively estimate the target state. When the Kalman filter is used, we assume that it does not have the knowledge whether the measurements are echos from the target or not. Thus, the filter assumes that the selected radars can always see the target, i.e., scenario 1 is always the case, and $\boldsymbol{H}_k(\mathcal{D}(\mathcal{U}_k))$ degenerates to $\boldsymbol{H}_k$. The procedures for the Kalman filter are summarized as follows:

$$\hat{\boldsymbol{x}}_{k|k-1} = \boldsymbol{A}_{k-1}\hat{\boldsymbol{x}}_{k-1|k-1}, \tag{12}$$

$$\boldsymbol{P}_{k|k-1} = \boldsymbol{A}_{k-1}\boldsymbol{P}_{k-1|k-1}\boldsymbol{A}_{k-1}^\top + \boldsymbol{V}_{k-1}, \tag{13}$$

$$\boldsymbol{K}_k = \boldsymbol{P}_{k|k-1}\boldsymbol{H}_k^\top(\boldsymbol{H}_k\boldsymbol{P}_{k|k-1}\boldsymbol{H}_k^\top + \boldsymbol{R}_k)^{-1}, \tag{14}$$

$$\hat{\boldsymbol{x}}_{k|k} = \hat{\boldsymbol{x}}_{k|k-1} + \boldsymbol{K}_k(\boldsymbol{z}_k - \boldsymbol{H}_k\hat{\boldsymbol{x}}_{k|k-1})), \tag{15}$$

$$\boldsymbol{P}_{k|k} = (\boldsymbol{I} - \boldsymbol{K}_k\boldsymbol{H}_k)\boldsymbol{P}_{k|k-1}, \tag{16}$$

where $\hat{\boldsymbol{x}}_{k|k-1}$ is the predicted state; $\boldsymbol{P}_{k|k-1}$ is the corresponding predicted covariance matrix; $\hat{\boldsymbol{x}}_{k|k}$ is the updated state; and $\boldsymbol{P}_{k|k}$ is the corresponding updated covariance matrix. In this case, $P(\boldsymbol{x}_k|\mathcal{Z}_{1:k-1})$ is Gaussian with mean $\hat{\boldsymbol{x}}_{k|k-1}$ and covariance matrix $\boldsymbol{P}_{k|k-1}$; while $P(\boldsymbol{x}_k|\mathcal{Z}_{1:k})$ is Gaussian with mean $\hat{\boldsymbol{x}}_{k|k}$ and covariance matrix $\boldsymbol{P}_{k|k}$, where $\mathcal{Z}_{1:k} = \{\mathcal{Z}_1, \ldots, \mathcal{Z}_k\}$ is the collection of the received measurements up to time k.

D. Cognitive Target Tracking Framework

We formulate the target tracking procedure as two iterative steps, i.e.,

$$\text{(i)} \quad \hat{\mathcal{D}}(\mathcal{U}_k) = \underset{\mathcal{D}(\mathcal{U}_k)}{\arg\max}\ f(\mathcal{D}(\mathcal{U}_k)) \quad \text{s.t.} \quad \mathcal{U}_k^s \in \Pi_k,\ \mathcal{U}_k^p \in \mathcal{L}_k, \tag{17}$$

$$\text{(ii)} \quad \hat{\boldsymbol{x}}_k = \underset{\boldsymbol{x}_k}{\arg\max}\ P(\boldsymbol{x}_k|\mathcal{Z}_{1:k}; \hat{\mathcal{D}}(\mathcal{U}_k)), \tag{18}$$

where step (i) solves a combinatorial optimization problem to select the optimal subset of radars $\mathcal{U}_k^s$ from the feasible set Π_k defined by resource constraints, and choose their locations $\mathcal{U}_k^p$ within the feasible set $\mathcal{L}_k$ restricted by the kinematic capabilities of radars. For example, Π_k can be the set that total c radars are used to track the target, and $\mathcal{U}_k^p$ can be the set that each radar moves within its predefined region. Step (ii) uses the RBSE technique (e.g., Kalman filter in this work) to update the state using the solution suggested by the step (i).

The function $f(\cdot)$ represents a well-designed objective function, and in this paper, we formulate $f(\cdot)$ as the expected negative cross-entropy, which measures the similarity between the predicted state distribution and the updated state distribution, i.e.,

$$f(\mathcal{D}(\mathcal{U}_k)) = \mathbb{E}_{p(\mathcal{Z}_k|\boldsymbol{x}_{k-1}=\hat{\boldsymbol{x}}_{k-1|k-1};\mathcal{D}(\mathcal{U}_k))}[-H_{\text{cross}}], \tag{19}$$

where the cross-entropy is computed at the output of the Kalman filter as

$$\begin{aligned} H_{\text{cross}} =& -\mathbb{E}_{p(\boldsymbol{x}_k|\mathcal{Z}_{1:k-1})}\log p(\boldsymbol{x}_k|\mathcal{Z}_{1:k}) \\ =& \frac{1}{2}\log(2\pi)^4 + \frac{1}{2}\log|\boldsymbol{P}_{k|k}| + \frac{1}{2}\text{tr}(\boldsymbol{P}_{k|k}^{-1}\boldsymbol{P}_{k|k-1}) \\ &+ \frac{1}{2}(\hat{\boldsymbol{x}}_{k|k} - \hat{\boldsymbol{x}}_{k|k-1})^\top\boldsymbol{P}_{k|k}^{-1}(\hat{\boldsymbol{x}}_{k|k} - \hat{\boldsymbol{x}}_{k|k-1}). \end{aligned} \tag{20}$$

Note that the expectation in (19) is nontrivial since two scenarios in (8) should be taken into account. Here we apply an approximation by dividing the continuous state space into finite discrete 4-D grids, i.e.,

$$\begin{aligned} & p(\mathcal{Z}_k|\boldsymbol{x}_{k-1} = \hat{\boldsymbol{x}}_{k-1|k-1}; \mathcal{D}(\mathcal{U}_k)) \\ &= \int p(\mathcal{Z}_k|\boldsymbol{x}_k; \mathcal{D}(\mathcal{U}_k))p(\boldsymbol{x}_k|\boldsymbol{x}_{k-1} = \hat{\boldsymbol{x}}_{k-1|k-1})d\boldsymbol{x}_k \\ &\approx \textstyle\sum_j p(\mathcal{Z}_k|\tilde{\boldsymbol{x}}_k^j; \mathcal{D}(\mathcal{U}_k))\frac{q_j}{C}, \end{aligned} \tag{21}$$

where $\tilde{\boldsymbol{x}}_k^j$ denotes the center of a discretized grid; C is a normalizing constant for the discrete probability distribution q_j; and

$$q_j = \int_{L(\tilde{\boldsymbol{x}}_k^j)} p(\boldsymbol{x}_k|\boldsymbol{x}_{k-1} = \hat{\boldsymbol{x}}_{k-1|k-1})d\boldsymbol{x}_k, \tag{22}$$

with $L(\tilde{\boldsymbol{x}}_k^j)$ is the grid having the center $\tilde{\boldsymbol{x}}_k^j$. We further assume that the velocity of the target does not significantly

$$f(\mathcal{D}(\mathcal{U}_k)) \approx \frac{1}{2}\log(2\pi)^4 + \frac{1}{2}\log|\boldsymbol{P}_{k|k}| + \frac{1}{2}\text{tr}(\boldsymbol{P}_{k|k}^{-1}\boldsymbol{P}_{k|k-1}) + \frac{1}{2}\text{tr}(\boldsymbol{K}_k^{\mathsf{T}}\boldsymbol{P}_{k|k}^{-1}\boldsymbol{K}_k\boldsymbol{R}_k)$$
$$+ \frac{1}{2C}\sum_j q_j \left(\boldsymbol{H}_k(\mathcal{D}(\mathcal{U}_k), \tilde{\boldsymbol{x}}_k)\tilde{\boldsymbol{x}}_k - \boldsymbol{H}_k\hat{\boldsymbol{x}}_{k|k-1}\right)^{\mathsf{T}} \boldsymbol{K}_k^{\mathsf{T}}\boldsymbol{P}_{k|k}^{-1}\boldsymbol{K}_k \left(\boldsymbol{H}_k(\mathcal{D}(\mathcal{U}_k), \tilde{\boldsymbol{x}}_k)\tilde{\boldsymbol{x}}_k - \boldsymbol{H}_k\hat{\boldsymbol{x}}_{k|k-1}\right) \quad (23)$$

change; thus the predicted velocity can be used for $\boldsymbol{x}_k$ in (22), and $L(\tilde{\boldsymbol{x}}_k^j)$ degenerates to a 2-D state space. Substituting (21) into (19), we have (23) as the objective function.

E. Compensation Rules

We introduce an intelligent rule to compensate for any imperfectness of the objective function. The objective function could be myopic or excessively rely on the current knowledge, resulting in an improper choice of the subset of radars and their locations. To avoid such issues we apply a compensation rule based on two distance metrics d_1 and d_2. At time $k-1$, we denote d_1 as the distance between positions of the updated state $\hat{\boldsymbol{x}}_{k-1|k-1}$ and the positions of the predicted state $\hat{\boldsymbol{x}}_{k|k-1}$; and denote d_2 as the distance between the positions of $\hat{\boldsymbol{x}}_{k-1|k-1}$ and the positions of the assumed updated state $\hat{\hat{\boldsymbol{x}}}_{k|k-1}$ of time k. This assumed updated state $\hat{\hat{\boldsymbol{x}}}_{k|k-1}$ is computed using the RBSE technique and an assumed set of collected measurements of time k if the solution of the combinatorial optimization problem is applied at time k. If d_2 is within some predefined thresholds, i.e., $\gamma_1 d_1 < d_2 < \gamma_2 d_1$, where $0 < \gamma_1 < 1 < \gamma_2$, then we accept the solution of the combinatorial optimization problem and apply it at time k. Otherwise, we randomly select a subset of radars and some locations where radars can see the target in the predicted state to replace the optimal solution.

In addition, we consider another rule to avoid the case in which received measurements contain only noise when the beams of selected radars do not cover the target (i.e., scenario 2 in (8)). After the radars receive the measurements at time k, we denote the distance between the positions of $\hat{\boldsymbol{x}}_{k|k}$ and the positions of $\hat{\boldsymbol{x}}_{k|k-1}$ as d_p, and the range resolution of radars as R_{res}. If $d_p > \gamma_p R_{\text{res}}$, where $\gamma_p > 0$, then the tracking filter gets a feedback that the beams of selected radars do not cover the target, and replace the output of step (ii) with the predicted state $\hat{\boldsymbol{x}}_{k|k-1}$.

III. Numerical Results

In this section, an illustrative example of the proposed framework in 2-D space is shown by Fig. 3, and the target tracking performance is demonstrated based on this example.

A. Simulation Setup

As shown in Fig. 3, there are J radars moving on the x and y axes, and all of them are sharing the same range-resolution R_{res}. The surveillance region is divided into several lattices by range resolutions. Each radar transmits the signal orthogonal to its moving direction, and its beam can cover only one row or column of the lattices. We assign each radar its own predefined surveillance space which consists of three contiguous columns or rows, and the assigned surveillance spaces of different radars are not overlapped if they are moving in the same direction. The path planning constraint $\mathcal{L}_k$ here is that radars cannot leave the regions corresponding to their assigned surveillance space. In addition, the union of the assigned surveillance regions of the radars moving in the same direction covers the entire workspace. In every tracking step, we set the radar selection constraint Π_k as that one radar on x axis and one radar on y axis are selected to track the target. The measurement collecting procedures are assumed to be independent.

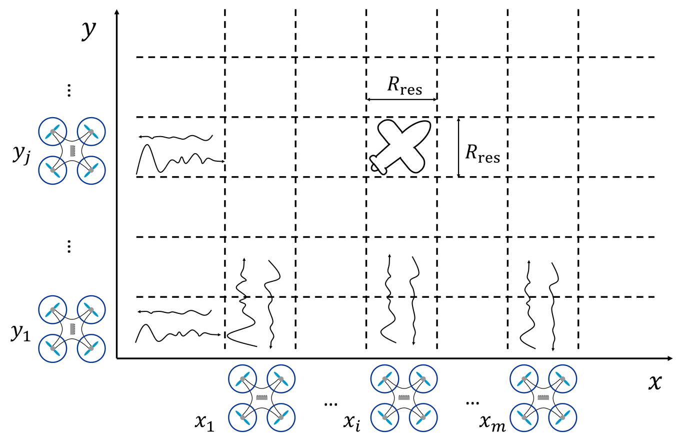

Fig. 3. Simulation setup of the illustrative example of the framework

In our simulation, we set the range resolution $R_{\text{res}} = 15$m, and the measurement noise covariance matrix $\boldsymbol{R}_k = \text{diag}(1,1,1,1)$. The initialization of the Kalman filter is considered as $\hat{\boldsymbol{x}}_{0|0} = [645, 150, 645, 150]^{\mathsf{T}}$, and $\boldsymbol{P}_{0|0} = \text{diag}(1, 0.1, 1, 0.1)$. For every Monte Carlo run, the initial true state is randomly sampled from a Gaussian distribution $\mathcal{N}(\hat{\boldsymbol{x}}_{0|0}, \boldsymbol{P}_{0|0})$, and total 30 runs with 60 tracking steps are used to compute the root-mean-squared error (RMSE) in the tracking performance. In (21), 5×5 grids (2-D) are used for the approximation. The parameters for compensation rules are given as $\gamma_1 = 0.75$, $\gamma_2 = 1.25$, and $\gamma_p = 2$. A grid searching method is used to solve the combinatorial optimization problem in the proposed framework.

B. Tracking Results

The target tracking performance is shown in Fig.4, with tracking time interval $T_{\text{in}} = 0.1$s and process noise intensities $q_1 = q_2 = 0.1$. We observe that the proposed framework is capable of robustly tracking a single target in the mobile radar network. In Fig. 4(a), the true trajectory of one Monte Carlo run is shown by the blue line, and the estimated (updated)

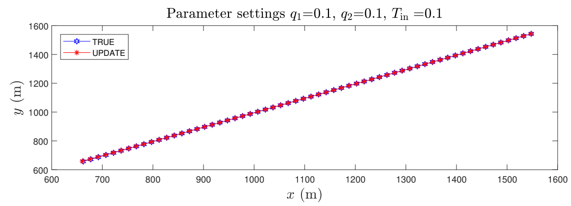

(a) True and estimated trajectories

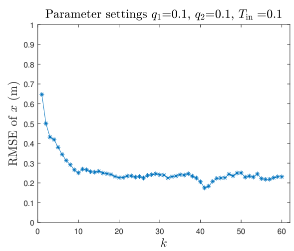

(b) RMSE of x

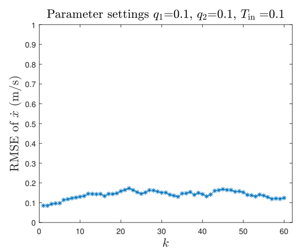

(c) RMSE of $\dot{x}$

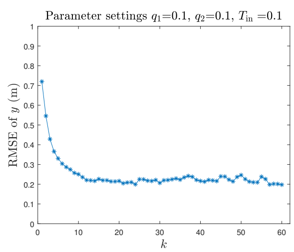

(d) RMSE of y

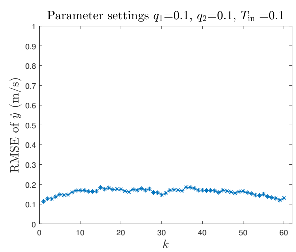

(e) RMSE of $\dot{y}$

Fig. 4. Tracking performance with the process noise intensities $q_1 = q_2 = 0.1$, and the tracking time-interval $T_{\rm in} = 0.1$ s. (a) Comparison of the true and estimated trajectories of the target, (b) root-mean-squared error (RMSE) of the position x, (c) RMSE of the velocity $\dot{x}$, (d) RMSE of the position y, (e) RMSE of the velocity $\dot{y}$.

trajectory by RBSE is shown by the red line. We see that these two trajectories are close to each other. From Figs. 4(b) and 4(d), we notice that the RMSEs of positions decrease during the tracking period. The RMSEs of velocities basically remain similar (see Figs. 4(c) and 4(e)); this is because only positions are measured by the radars and new noise is added to perturb the velocities in the kinematic model at every tracking step.

IV. Conclusions and Future Work

In this paper, we proposed a framework of single target tracking via a radar network, jointly considering radar selection and path planning. Based on the dynamic graphical model and recursive Bayesian state estimation techniques, we formulated the tracking procedure as alternately solving a combinatorial optimization problem and recursively estimating the target state. We demonstrated the proposed framework using an illustrative example, and achieved good target tracking performance on the simulation. However, in this work, only expected negative cross-entropy was considered for the objective function, which may lead to an incomplete exploration and exploitation of the environmental information. Therefore, in our future work, we will extend the framework to investigate other objective functions, to balance the strengths and weaknesses of them, and to solve a multi-objective optimization problem for building up non-myopic policies. In addition, we will testify the proposed framework on more complicated and practical scenarios.

References

[1] A. O. Hero and D. Cochran, "Sensor management: past, present, and future," *IEEE Sensors Journal*, vol. 11, no. 12, pp. 3064–3075, 2011.
[2] S. Haykin, "Cognitive radar: a way of the future," *IEEE signal processing magazine*, vol. 23, no. 1, pp. 30–40, 2006.
[3] K. L. Bell, C. J. Baker, G. E. Smith, J. T. Johnson, and M. Rangaswamy, "Cognitive radar framework for target detection and tracking," *IEEE Journal of Selected Topics in Signal Processing*, vol. 9, no. 8, pp. 1427–1439, Dec. 2015.
[4] S. Joshi and S. Boyd, "Sensor selection via convex optimization," *IEEE Transactions on Signal Processing*, vol. 57, no. 2, pp. 451–462, 2009.
[5] M. Shamaiah, S. Banerjee, and H. Vikalo, "Greedy sensor selection: Leveraging submodularity," in *49th IEEE Conference on Decision and Control (CDC)*, 2010, pp. 2572–2577.
[6] P. Chavali and A. Nehorai, "Scheduling and power allocation in a cognitive radar network for multiple-target tracking," *IEEE Transactions on Signal Processing*, vol. 60, no. 2, pp. 715–729, 2012.
[7] N. Cao, S. Choi, E. Masazade, and P. K. Varshney, "Sensor selection for target tracking in wireless sensor networks with uncertainty," *IEEE Transactions on Signal Processing*, vol. 64, no. 20, pp. 5191–5204, 2016.
[8] X. Shen and P. K. Varshney, "Sensor selection based on generalized information gain for target tracking in large sensor networks," *IEEE Transactions on Signal Processing*, vol. 62, no. 2, pp. 363–375, 2014.
[9] M. Xie, W. Yi, and L. Kong, "Joint node selection and power allocation for multitarget tracking in decentralized radar networks," in *19th International Conference on Information Fusion (FUSION)*, 2016, pp. 45–52.
[10] A. S. Narykov, O. A. Krasnov, and A. Yarovoy, "Algorithm for resource management of multiple phased array radars for target tracking," in *Proceedings of the 16th International Conference on Information Fusion (ISIF)*, 2013, pp. 1258–1264.
[11] G. Zhang, S. Ferrari, and M. Qian, "An information roadmap method for robotic sensor path planning," *Journal of Intelligent and Robotic Systems*, vol. 56, no. 1, pp. 69–98, Sep. 2009.
[12] K. Dogancay, "UAV path planning for passive emitter localization," *IEEE Transactions on Aerospace and Electronic systems*, vol. 48, no. 2, pp. 1150–1166, 2012.
[13] ——, "Single-and multi-platform constrained sensor path optimization for angle-of-arrival target tracking," in *18th European Signal Processing Conference (EUSIPCO)*, 2010, pp. 835–839.
[14] Y. Oshman and P. Davidson, "Optimization of observer trajectories for bearings-only target localization," *IEEE Transactions on Aerospace and Electronic Systems*, vol. 35, no. 3, pp. 892–902, 1999.
[15] K. Zhou and S. I. Roumeliotis, "Optimal motion strategies for range-only constrained multisensor target tracking," *IEEE Transactions on Robotics*, vol. 24, no. 5, pp. 1168–1185, 2008.
[16] B. Grocholsky, A. Makarenko, and H. Durrant-Whyte, "Information-theoretic coordinated control of multiple sensor platforms," in *IEEE International Conference on Robotics and Automation (ICRA)*, vol. 1, 2003, pp. 1521–1526.
[17] S. A. Miller, Z. A. Harris, and E. K. Chong, "A POMDP framework for coordinated guidance of autonomous uavs for multitarget tracking," *EURASIP Journal on Advances in Signal Processing*, vol. 2009, no. 1, p. 724597, Jan. 2009.
[18] N. H. Nguyen and K. Doğançay, "Optimal sensor placement for Doppler shift target localization," in *IEEE Radar Conference (RadarCon)*, 2015, pp. 1677–1682.
[19] M. Hurtado and A. Nehorai, "Bat-inspired adaptive design of waveform and trajectory for radar," in *42nd Asilomar Conference on Signals, Systems and Computers (ASILOMAR)*, 2008, pp. 36–40.
[20] Y. Bar-Shalom, X. R. Li, and T. Kirubarajan, *Estimation with Applications to Tracking and Navigation: Theory algorithms and Software*. John Wiley & Sons, 2004.